Low Wall Shear Stress Is Independently Associated With the Rupture Status of Middle Cerebral Artery Aneurysms

Yoichi Miura, MD; Fujimaro Ishida, MD; Yasuyuki Umeda, MD; Hiroshi Tanemura, MD; Hidenori Suzuki, MD; Satoshi Matsushima, MD; Shinichi Shimosaka, MD; Waro Taki, MD

Background and Purpose—We determined which hemodynamic parameter independently characterizes the rupture status of middle cerebral artery (MCA) aneurysms using computational fluid dynamics analysis.

Methods—In 106 patient-specific geometries of MCA aneurysms (43 ruptured, 63 unruptured), morphological and hemodynamic parameters were compared between the ruptured and unruptured groups. Multivariate logistic regression analysis was performed to determine parameters that independently characterized the rupture status of MCA aneurysms.

Results—Univariate analyses showed that the aspect ratio, wall shear stress (WSS), normalized WSS, oscillatory shear index, WSS gradient, and aneurysm-formation index were significant parameters. The size of the aneurysmal dome and the gradient oscillatory number were not significantly different between the 2 groups. With multivariate analyses, only lower WSS was significantly associated with the rupture status of MCA aneurysms.

Conclusions—WSS may be the most reliable parameter characterizing the rupture status of MCA aneurysms. **(*Stroke*. 2013;44:519-521.)**

Key Words: computational fluid dynamics analysis ■ middle cerebral artery aneurysm ■ wall shear stress

Recent studies using computational fluid dynamics techniques have demonstrated that hemodynamic features may be key parameters for understanding cerebral aneurysm rupture.[1,2] However, previous computational fluid dynamics studies simultaneously evaluated only a limited number of hemodynamic parameters in a relatively small number of patient-specific geometries, which included different locations of the aneurysm; this may be one reason why some findings are conflicting.

The current study focused on only MCA aneurysms. We used computational fluid dynamics to simultaneously analyze different hemodynamic parameters and determine which parameter independently characterizes the rupture status of MCA aneurysms.

Methods

One hundred and six saccular MCA aneurysms (43, ruptured; 63, unruptured) diagnosed with 3-dimensional rotational angiography were analyzed. The patient-specific geometries were reconstructed from 3-dimensional rotational angiography images. Computational fluid dynamics simulations were performed under pulsatile flow conditions driven from typical blood-flow waveforms of the common carotid artery in normal humans,[3] and the following hemodynamic parameters were calculated: wall shear stress (WSS), normalized WSS (NWSS),[2] oscillatory shear index (OSI),[4] WSS gradient (WSSG),[5] gradient oscillatory number,[6] and aneurysm-formation indicator (AFI).[7] Morphological (aneurysm size and aspect ratio) and hemodynamic parameters were compared between ruptured and unruptured aneurysms (see expanded methods in the online only data supplement).

Results

Univariate Analysis

As not all morphological and hemodynamic parameters were normally distributed, they were analyzed with the Wilcoxon rank-sum test (Table 1).

The median of the size of the aneurysmal dome and the aspect ratio were 5.36 mm and 1.43, respectively, for ruptured aneurysms, and 5.30 mm and 1.33, respectively, for unruptured aneurysms. There was no significant difference in the size of the aneurysmal dome (P=0.122), whereas the aspect ratio was significantly different (P=0.0298).

Distributions of WSS, OSI, WSSG, gradient oscillatory number, and AFI for ruptured and unruptured aneurysms are shown in Figure. Ruptured aneurysms had significantly lower WSS, lower NWSS, higher OSI, lower WSSG, and lower AFI than unruptured aneurysms (7.19 Pa versus 9.55 Pa, P=0.00010; 0.490 versus 0.618, P=0.0129; 0.0165 versus 0.0125, P=0.00891; 7.15 Pa/mm versus 10.40 Pa/mm, P=0.00020; and 0.971 versus 0.978, P=0.00631, respectively).

Received September 3, 2012; final revision received October 1, 2012; accepted October 16, 2012.

From the Department of Neurosurgery, Mie University Graduate School of Medicine, Tsu, Japan (Y.M., Y.U., H.S., S.M., W.T.) and the Department of Neurosurgery, Mie Chuo Medical Center, National Hospital Organization, Tsu, Japan (F.I., H.T., S.S.).

The online-only Data Supplement is available with this article at http://stroke.ahajournals.org/lookup/suppl/doi:10.1161/STROKEAHA.112.675306/-/DC1.

Correspondence to Fujimaro Ishida, MD, Department of Neurosurgery, Mie Chuo Medical Center, National Hospital Organization, 2158-5 Hisai-Myojin Cho, Tsu City, Mie 514-1101, Japan. E-mail nsfuji@me.com

Table 1. Summary of Morphological and Hemodynamic Parameters for Ruptured and Unruptured MCA Aneurysms

Parameter	Ruptured (n=43)	Unruptured (n=63)	*P* Value*
Size, mm	5.36 (3.97–7.80)	5.30 (3.99–7.27)	0.122
Aspect ratio	1.43 (1.14–1.77)	1.33 (1.06–1.64)	0.0298
WSS, Pa	7.19 (3.54–11.61)	9.55 (5.72–13.67)	0.00010
NWSS	0.490 (0.291–0.813)	0.618 (0.340–0.851)	0.0129
OSI	0.0165 (0.0110–0.0308)	0.0125 (0.00871–0.0230)	0.00891
WSSG, Pa/mm	7.15 (3.91–14.15)	10.40 (5.97–15.56)	0.00020
GON	0.0593 (0.0420–0.0899)	0.0578 (0.0402–0.0828)	0.180
AFI	0.971 (0.935–0.990)	0.978 (0.957–0.992)	0.00631

AFI indicates aneurysm formation indicator; GON, gradient oscillatory number; NWSS, normalized WSS; OSI, oscillatory shear index; WSS, wall shear stress; and WSSG, WSS gradient.

Values are the median (interquartile range).

*Wilcoxon rank-sum test.

Gradient oscillatory number was not significantly different between the 2 groups (P=0.180).

Intercorrelations Among Parameters

Intercorrelations between significant parameters with univariate analyses were examined using Spearman's rank correlation test. WSS was significantly correlated with NWSS (correlation coefficient: R=0.8022, P<0.0001, coefficient of determination: R^2=0.644) and WSSG (R=0.8743, P<0.0001, R^2=0.764). Other parameters were not significantly correlated (R<0.6).

Multivariate Analyses

Because WSS had the lowest P value in the Wilcoxon rank-sum test among WSS, NWSS, and WSSG, which were significantly correlated, only WSS was used as a candidate variable. Thus, the aspect ratio, WSS, OSI, and AFI, which were significant with univariate analyses, were considered independent variables (Table 2). With multivariate logistic regression analyses, only WSS was significantly associated with the rupture status (OR: 0.929; 95% CI: 0.850–0.992; P=0.0227).

From analysis of the receiver-operating characteristic curve for WSS, the area under the curve was 0.723, and the cut-off value was 7.263, with a sensitivity of 0.698 and a specificity of 0.698 (Figure I in the online-only Data Supplement).

Discussion

This study showed that not only the aspect ratio, but also WSS and some WSS-related hemodynamic parameters, such as NWSS, OSI, WSSG, and AFI, were significantly different between ruptured and unruptured MCA aneurysms. Moreover, the most important finding is the first demonstration that only WSS is an independent factor for characterizing the rupture status of MCA aneurysms.

There are 2 theories explaining the mechanisms of cerebral aneurysm rupture: high- and low-flow theories.[8,9] Consistent with these theories, previous computational fluid dynamics studies reported different findings regarding the rupture status of cerebral aneurysms. Cebral et al[1] reported that ruptured aneurysms have higher WSS compared with unruptured aneurysms in 210 aneurysms, but they provided no information about the location and size. Xiang et al[2] analyzed 119 aneurysms in various locations and reported that ruptured aneurysms have a lower WSS and higher OSI. Because aneurysm location may affect computational fluid dynamic findings, this study simultaneously determined various hemodynamic parameters only in MCA aneurysms, using a statistically reasonable number of patient-specific geometries. As a result, the results of this study support the low-flow theory. In addition, this study is the first to demonstrate that lower WSSG and lower AFI were significantly correlated with the rupture status of cerebral aneurysms. Previous studies demonstrated that OSI is

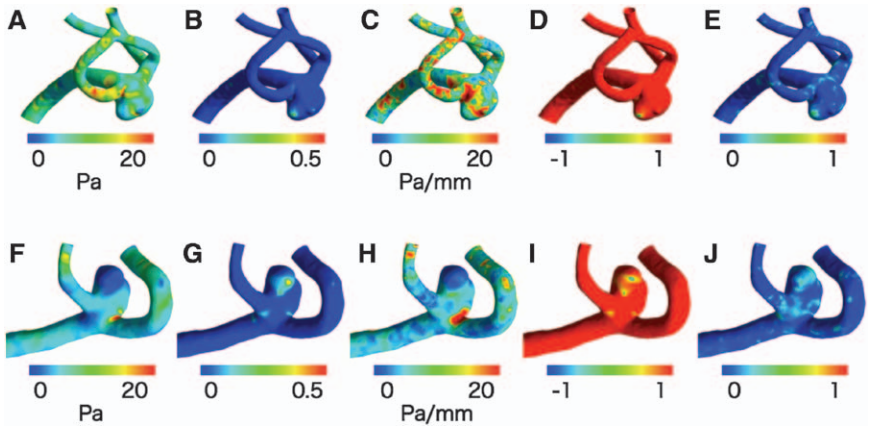

Figure. Wall shear stress (**A** and **F**), oscillatory shear index (**B** and **G**), WSS gradient (**C** and **H**), gradient oscillatory number (**D** and **I**), and aneurysm-formation indicator (**E** and **J**) of representative middle cerebral artery aneurysms (upper, unruptured; lower, ruptured).

Table 2. Multivariate Logistic Regression Analysis of Independent Parameters Associated With the Rupture Status of MCA Aneurysms

Independent Parameters	OR†	95% CI	*P* Value‡
Aspect ratio	1.521	0.695 to 3.508	0.2952
WSS	0.929	0.850 to 0.992	0.0227
OSI	0.0143	1.08e–18 to 4.5e+8	0.7387
AFI	0.0232	0.695 to 54.505	0.2438

AFI indicates aneurysm formation indicator; CI, confidence interval; OR, odds ratio; OSI, oscillatory shear index; and WSS, wall shear stress.

A *P*-value <0.05 was considered statistically significant.

†Estimated OR of association with a 1-point increase in the independent variable.

‡Multivariate logistic regression analysis.

associated with complex flow,[4] and WSSG is associated with disrupted flow and intimal hyperplasia.[5] In contrast, AFI could detect stagnation zones, and low AFI was found in the location where the aneurysm formed.[6] Therefore, our results suggest that intra-aneurysmal flow stagnation and complex flow may be linked to aneurysm rupture, at least in MCA aneurysms.

This article has several limitations. First, blood was modeled as a Newtonian fluid with a fixed density and viscosity, and vessel wall was considered to be rigid. Although previous computational fluid dynamic studies reported that the assumptions limitedly affected the hemodynamics,[10] it would be worthwhile to examine effects of the assumptions on hemodynamic parameters, especially in patients with smoking, a well-known risk factor for aneurysm rupture. Second, this study did not take aneurysm histology, or physiological and humoral parameters into account. Third, in this study, only WSS distinguished the rupture status of MCA aneurysms in multivariate analyses, but the results cannot be extrapolated to other sites of aneurysms that may have different hemodynamics. Forth, this is a retrospective study that is potentially biased. Lastly, ruptured aneurysms can undergo some structural changes during and after the rupture, which affect the hemodynamics. Thus, the hemodynamic features in a ruptured aneurysm may differ from that of the aneurysm just before the rupture. A large-scale prospective cohort study of unruptured aneurysms should be performed to characterize the hemodynamics of unruptured aneurysms that eventually rupture and those that do not, taking account of many factors, including physiological and humoral parameters that may affect the results. This would be an important step to determine if intra-aneurysmal flow dynamics is useful to predict the individual risk of rupture of unruptured aneurysms.

Conclusions

In the largest population examined thus far, this study demonstrated that WSS may be the most reliable indicator for discriminating the rupture status of MCA aneurysms. To confirm whether this finding is a cause, result, or mere epiphenomenon of an aneurysm rupture requires further studies.

Disclosures

None.

References

1. Cebral JR, Mut F, Weir J, Putman C. Quantitative characterization of the hemodynamic environment in ruptured and unruptured brain aneurysms. *AJNR Am J Neuroradiol*. 2011;32:145–151.
2. Xiang J, Natarajan SK, Tremmel M, Ma D, Mocco J, Hopkins LN, et al. Meng H. Hemodynamic-morphologic discriminants for intracranial aneurysm rupture. *Stroke*. 2011;42:144–152.
3. Holdsworth DW, Norley CJ, Frayne R, Steinman DA, Rutt BK. Characterization of common carotid artery blood-flow waveforms in normal human subjects. *Physiol Meas*. 1999;20:219–240.
4. Taylor CA, Hughes TJ, Zarins CK. Finite element modeling of three-dimensional pulsatile flow in the abdominal aorta: relevance to atherosclerosis. *Ann Biomed Eng*. 1998;26:975–987.
5. Lei M, Kleinstreuer C, Truskey GA. A focal stress gradient-dependent mass transfer mechanism for atherogenesis in branching arteries. *Med Eng Phys*. 1996;18:326–332.
6. Shimogonya Y, Ishikawa T, Imai Y, Matsuki N, Yamaguchi T. Can temporal fluctuation in spatial wall shear stress gradient initiate a cerebral aneurysm? A proposed novel hemodynamic index, the gradient oscillatory number (GON). *J Biomech*. 2009;42:550–554.
7. Mantha A, Karmonik C, Benndorf G, Strother C, Metcalfe R. Hemodynamics in a cerebral artery before and after the formation of an aneurysm. *AJNR Am J Neuroradiol*. 2006;27:1113–1118.
8. Nakatani H, Hashimoto N, Kang Y, Yamazoe N, Kikuchi H, Yamaguchi S, et al. Cerebral blood flow patterns at major vessel bifurcations and aneurysms in rats. *J Neurosurg*. 1991;74:258–262.
9. Boussel L, Rayz V, McCulloch C, Martin A, Acevedo-Bolton G, Lawton M, et al. Aneurysm growth occurs at region of low wall shear stress: patient-specific correlation of hemodynamics and growth in a longitudinal study. *Stroke*. 2008;39:2997–3002.
10. Cebral JR, Castro MA, Appanaboyina S, Putman CM, Millan D, Frangi AF. Efficient pipeline for image-based patient-specific analysis of cerebral aneurysm hemodynamics: technique and sensitivity. *IEEE Trans Med Imaging*. 2005;24:457–467.

Low Wall Shear Stress Is Independently Associated With the Rupture Status of Middle Cerebral Artery Aneurysms

Yoichi Miura, Fujimaro Ishida, Yasuyuki Umeda, Hiroshi Tanemura, Hidenori Suzuki, Satoshi Matsushima, Shinichi Shimosaka and Waro Taki

Stroke. 2013;44:519-521; originally published online December 6, 2012;
doi: 10.1161/STROKEAHA.112.675306
Stroke is published by the American Heart Association, 7272 Greenville Avenue, Dallas, TX 75231

Print ISSN: 0039-2499. Online ISSN: 1524-4628

SUPPLEMENTAL MATERIAL

Supplemental Methods

Data Source

From April 2007 to March 2011, one hundred and six MCA aneurysms from 88 patients diagnosed with 3D rotational angiography were analyzed in this study. Of these aneurysms, 43 were ruptured and 63 were unruptured. Patients ranged from 33 to 84 years of age, with a mean age of 63 years. All aneurysms were saccular aneurysms originating at the first major bifurcation of the MCA; saccular aneurysms that formed at other portions of the MCA, fusiform or dissecting aneurysms, and aneurysms associated with cerebral vasospasm were excluded. In patients with SAH and multiple cerebral aneurysms, a ruptured aneurysm was diagnosed by clinical and radiological findings and was confirmed by operative findings.

Image Acquisition

All cerebral angiograms were performed with standard transfemoral approaches. The patient-specific geometries were reconstructed from three-dimensional rotational angiography images (Allura Xper FD20, Philips Medical Systems, Best, the Netherlands). Fast rotational angiography was performed with a 240-degree rotation of the C-arm in 4.4 sec. The exposure was 30 frames/sec, and the flat panel detector was set to 8 inches. The first rotation provided the subtraction mask. The second rotation was performed simultaneously with the administration of contrast material. Twenty-four milliliters of contrast material was injected into the cervical internal carotid artery at 3.5 ml/sec via a selectively positioned catheter.

Morphological variables

For each aneurysm, the neck width and the maximum height of the aneurysmal dome were measured from 3D rotational angiography images and the aspect ratio was determined as the maximum distance of dome/width of the neck of an aneurysm.[1]

Model Construction

The surface of the arterial lumen was first constructed using a commercially available software package (Magics 13.0; Materialise Japan, Yokohama, Japan). The computational meshes were generated for these models using commercial software (ANSYS ICEM CFD12.1, ANSYS Inc., Canonsburg, PA, USA). The minimum element size was 0.1 mm, with smaller elements in high curvature regions. Three prismatic boundary layers with a total thickness of 0.15 mm covered the vessel wall to locally ensure an accurate definition of the velocity gradient. A straight inlet extension was added to the C5 segment of the internal carotid artery to obtain fully developed laminar flow. On average, computational meshes consisted of 290,000 nodes and 740,000 tetrahedral and prismatic elements.

Numerical Modeling

For the fluid domain, three-dimensional steady incompressible laminar flow fields were obtained by solving the continuity and Navier-Stokes equations. Numerical modeling was performed using a commercially available computational fluid dynamics package (ANSYS CFX12.1, ANSYS Inc.). Vessel walls were assumed to be rigid, and no slip boundary conditions were applied at the walls. Blood was assumed to be an incompressible Newtonian fluid with a blood density of 1056 kg/m^3 and blood viscosity of 0.0035 N/m^2 per second. Pulsatile boundary conditions of flow were based on the superposition of typical blood-flow waveforms of the common carotid artery by Doppler ultrasound in normal humans for a transient analysis.[2] Traction-free boundary conditions were applied at outlets of the middle cerebral artery and anterior cerebral artery. The width of the time step for calculation was set at 0.001 sec. To confirm numerical stability, we computed two cardiac cycles, and data from the second cardiac cycle were analyzed.

Hemodynamic Parameters

From the simulated flow fields, we calculated the following 6 hemodynamic parameters.

The concept of wall shear stress (WSS) refers to the tangential, frictional stress exerted by the action of blood flow on the vessel wall. WSS values were recorded at the aneurysmal dome. For pulsatile flow, the time-averaged WSS was calculated by integrating the WSS magnitude at each geometric part over the cardiac cycle:

$$WSS = \frac{1}{T}\int_0^T \left| wss_i \right| dt$$

where wss_i is the instantaneous WSS vector and T is the duration of the cycle.

Normalized WSS (NWSS) was defined as the WSS ratio to the WSS magnitude of the parent artery. WSS distributions were normalized to the average parent vessel WSS in the same patient to allow comparison of WSS magnitude among different patients.[3]

Oscillatory shear index (OSI) measured the directional change of WSS during the cardiac cycle.[4] OSI identified regions of high cyclic departure of the WSS vector from its predominant axial alignment over the cardiac cycle. OSI was defined as OSI averaged over the aneurysmal dome:

$$OSI = \frac{1}{2}\left(1 - \frac{\left|\int_0^T wss_i \, dt\right|}{\int_0^T \left|wss_i\right| dt}\right)$$

WSS gradient (WSSG) was calculated by taking the spatial derivative of WSS.[5] WSSG was the parameter that indicated the state of disrupted flow. WSSG was defined as the magnitude of time-averaged WSSG over the aneurysmal dome.

$$WSSG = \sqrt{\left(\frac{\partial \boldsymbol{\tau}_{w,p}}{\partial p}\right)^2 + \left(\frac{\partial \boldsymbol{\tau}_{w,q}}{\partial q}\right)^2}$$

where τ_w is the WSS vector, the *p*-direction corresponds to the time-averaged direction of the WSS, and the *q*-direction is perpendicular to *p*.

Gradient oscillatory number (GON) measured fluctuations in the WSS gradient integrated over one cardiac cycle to quantify the degree of oscillating tension/compression forces on endothelial cells. GON was defined as GON averaged over the aneurysmal dome:[6]

$$GON = 1 - \frac{\left| \int_0^T wssg_i \, dt \right|}{\int_0^T \left| wssg_i \right| dt}$$

where $wssg_i$ is the instantaneous WSS gradient vector and T is the duration of the cycle.

Aneurysm formation index (AFI) was an index to detect the flow stagnation zones. AFI was defined as AFI averaged over the aneurysmal dome at mid-systole:[7]

$$AFI = \cos(\theta) = \frac{wss_i \cdot wss}{\left| wss_i \right| * \left| wss \right|}$$

where *wss* is the time-averaged WSS.

Statistical Analysis

All data were analyzed using JMP 9 (SAS Institute Inc., Cary, NC, USA). The Anderson-Darling test was performed to assess the normal distribution of the population. Univariate analyses were performed with a Wilcoxon rank-sum test for each parameter between the ruptured and unruptured groups. Inter-correlations between parameters were examined using Spearman's rank correlation test. The impact of each parameter on the rupture status was determined by multivariate logistic regression analyses using the dichotomous status (ruptured or unruptured) as the dependent variable. Adjusted odds ratios (OR) with 95% confidence intervals (CI) were calculated, and independence of variables was tested using the likelihood ratio test on reduced models. P values less than 0.05 were considered significant.

Supplemental Reference

1. Weir B, Amidei C, Kongable G, Findlay JM, Kassell NF, Kelly J, et al. The aspect ratio (dome/neck) of ruptured and unruptured aneurysms. *J Neurosurg.* 2003;99:447-451.
2. Holdsworth DW, Norley CJ, Frayne R, Steinman DA, Rutt BK. Characterization of common carotid artery blood-flow waveforms in normal human subjects. *Physiol Meas.* 1999;20:219-240.
3. Jou LD, Lee DH, Morsi H, Mawad ME. Wall shear stress on ruptured and unruptured intracranial aneurysms at the internal carotid artery. *AJNR Am J Neuroradiol*. 2008;29:1761-1767.
4. Taylor CA, Hughes TJ, Zarins CK. Finite element modeling of three-dimensional pulsatile flow in the abdominal aorta: Relevance to atherosclerosis. *Ann Biomed Eng.* 1998;26:975-987.
5. Lei M, Kleinstreuer C, Truskey GA. A focal stress gradient-dependent mass transfer

mechanism for atherogenesis in branching arteries. *Med Eng Phys.* 1996;18:326-332.
6. Shimogonya Y, Ishikawa T, Imai Y, Matsuki N, Yamaguchi T. Can temporal fluctuation in spatial wall shear stress gradient initiate a cerebral aneurysm? A proposed novel hemodynamic index, the gradient oscillatory number (GON). *J Biomech.* 2009;42:550-554.
7. Mantha A, Karmonik C, Benndorf G, Strother C, Metcalfe R. Hemodynamics in a Cerebral Artery before and after the Formation of an Aneurysm. *AJNR Am J Neuroradiol.* 2006;27:1113-1118.

Supplemental Figure and Figure Legend

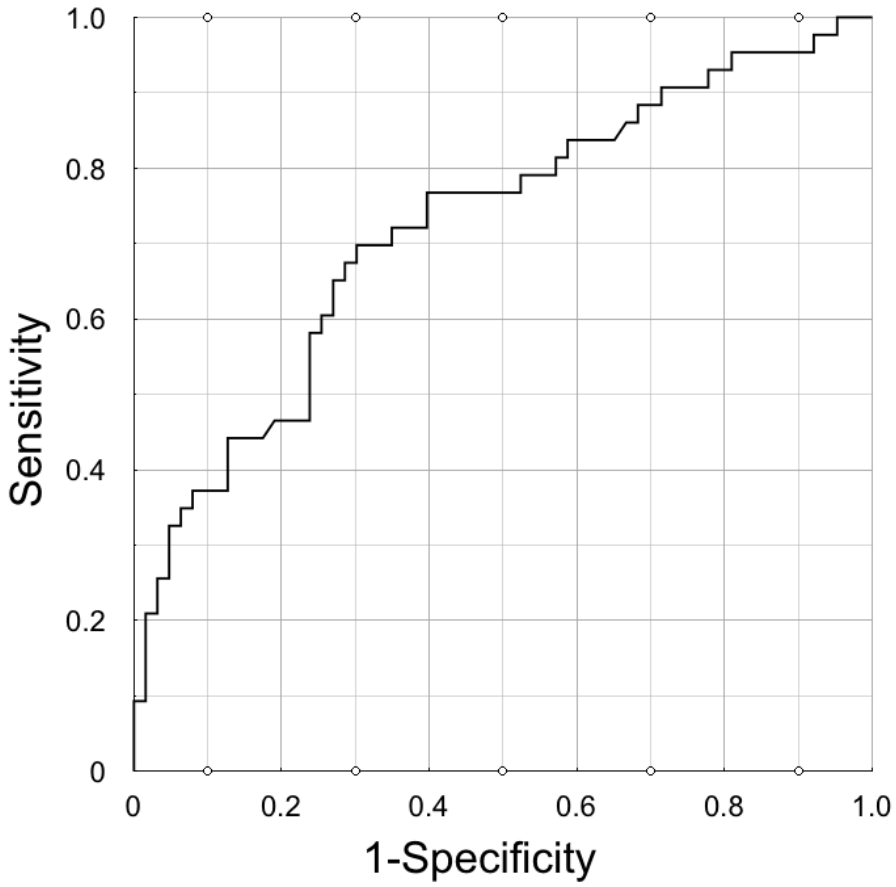

Figure S1. The receiver operating characteristic curve to determine WSS cut-off value for discrimination of MCA aneurysm rupture. The area under the curve is 0.723, and the cut-off value is 7.263, with a sensitivity of 0.698 and a specificity of 0.698.